Chapter 2 Hydrogen Plasma Passivation Effects on GaAs Epilayer Grown on Si Substrate

2. 1 Introduction

GaAs and related compound semiconductor heteroepitaxial layers on Si substrate have received considerable interest because it opens a way to integrate the superior properties of the compound semiconductors with the mature technology of silicon.[1, 2] As described in chapter 1, to improve the quality of the GaAs on Si layers, several attempts have been made[3], such as, growth of low temperature nucleation layers[4] and strained layer superlattice as buffer layers[5], thermal cycle growth[6], etc. Though these efforts improved the crystallinity of the heterostructure to some extent, dislocation density is still much higher (~10^6 cm^{-2}) than that is acceptable (~10^4 cm^{-2}) for practical applications. Since the generation of defects in GaAs on Si epilayers can not be avoided to the full extent, passivation of the activity of these defects is very essential. In the past, passivation of a wide range of shallow and deep impurities in the semiconductor by hydrogen incorporation was extensively investigated.[7- 9] More recently, the H passivation effect on electrical properties of the GaAs on Si has been reported.[10, 11] However, to our knowledge, the effects of H passivation on the optical properties is not well studied, so far.

In this chapter, we present the effects of plasma hydrogenation on the optical and electrical properties of GaAs epitaxial layers (GaAs/Si) and AlGaAs/GaAs multiple quantum well (MQW) grown on Si substrate, which are characterized by capacitance-voltage (C-V), photoluminescence (PL), and deep-level transient spectra (DLTS) methods. In addition, the annealing effects on the H_2 plasma passivated GaAs/Si epilayers are also presented. The organization of this chapter is as follows: In section 2.2, the growth of GaAs epilayers on Si and the RF plasma equipment used in the present experiment are described. The GaAs epilayer and the change induced by H_2 plasma

passivation on physical properties are characterized in chapter 2. 3. Chapter 2. 4 describes the hydrogen plasma passivation effects on AlGaAs/GaAs MQW on Si. Finally, this chapter is summarized in section 2. 5.

2. 2 Experimental procedure

2 . 2. 1 Epitaxial growth of GaAs using low pressure MOCVD

The samples have been grown by the low pressure (76 Torr) metal-organic chemical vapor deposition (MOCVD) using two-step growth technique. Figure 2.1 shows the schematic illustration of the low pressure MOCVD system used in this growth.

The system may be grouped into four major components:

(1) The gas handling system, including the hydrides and metalorganics source, valves, plumbing, H_2 purification equipment and instruments necessary to control gas flow and mixture.

(2) The reactor chamber in which the deposition occurs and the radio frequency (RF) plasma exposure is performed.

(3) Infrared ray (IR) lamp unit heating system.

(4) The exhaust or low pressure pumping system.

The source materials for Ga and As are trimethylgallium and AsH_3 diluted to 10 % in hydrogen (H_2) , respectively. Si substrate with an orientation of (001), tilted 4° toward [110], was used. The substrate was etched in aqueous solution of HF, and thermally cleaned at 1000°C for 10 min., followed by the growth of a thin GaAs buffer layer at 400°C. Then a 3 μm thick GaAs top layer was grown at 750°C. All the unintentionally doped GaAs layers were n-type and the full width at half maximum (FWHM) of the double-crystal x-ray diffraction were around 180 arcsec.

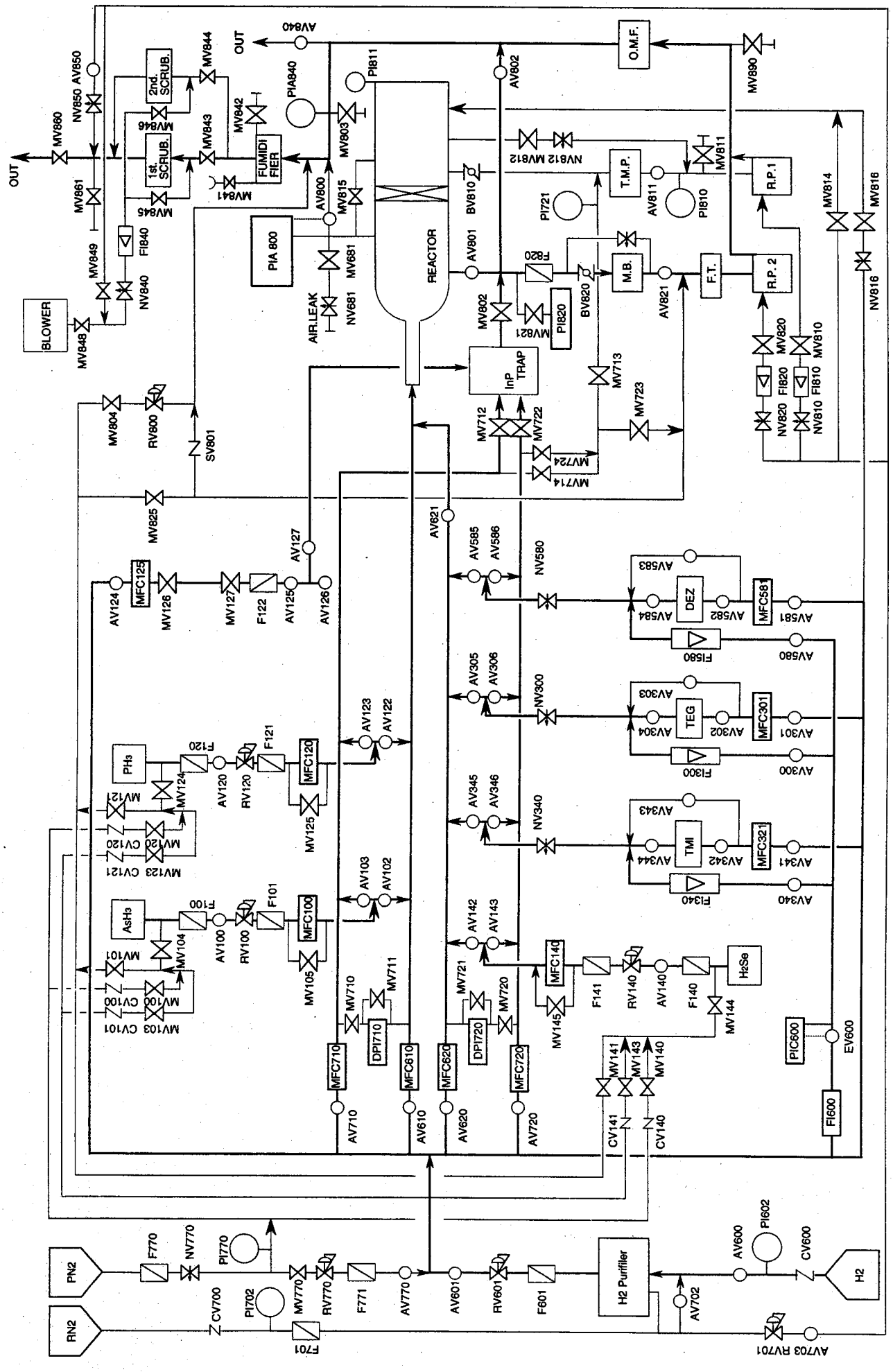

Fig. 2. 1 Schematic illustration of the low pressure MOCVD system.

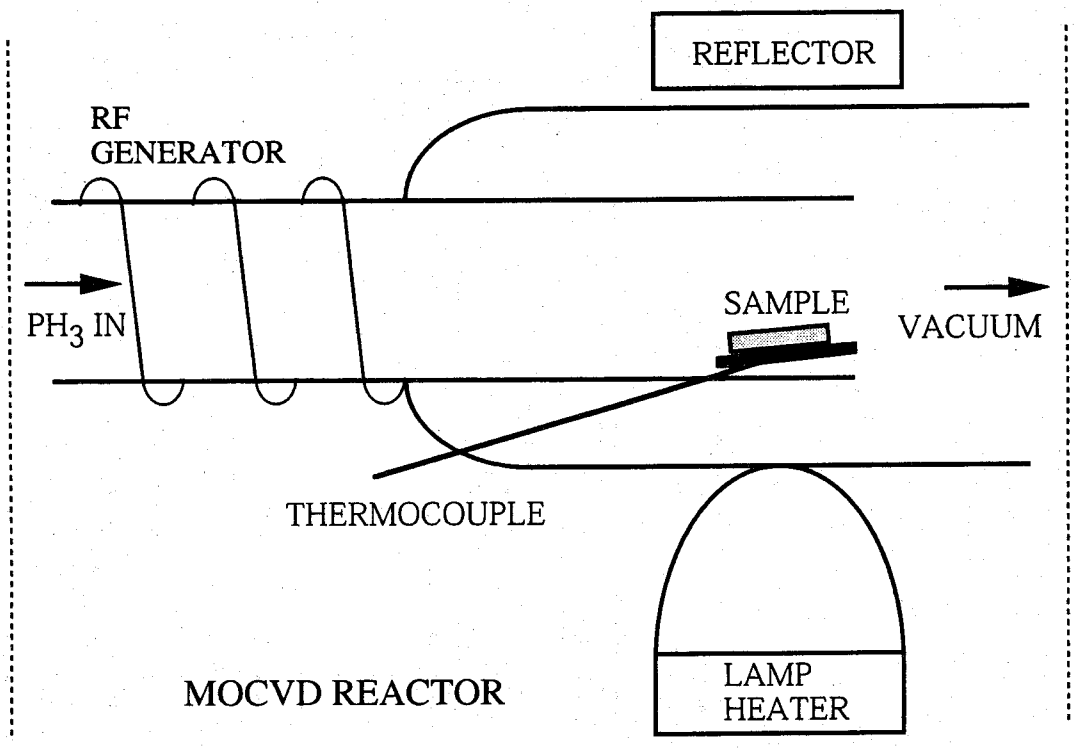

Fig. 2. 2 The schematic illustration reactor chamber of the MOCVD.

2. 2. 2 H_2 plasma exposure for GaAs epilayer on Si

Figure 2. 2 shows the reactor chamber in which the deposition occurs. The passivation is also carried out in it through which molecular hydrogen is pumped at a reduced pressure (0.1Torr). The hydrogen plasma is excited by radio-frequency (13.56 MHz) power via a copper coil encircling the quartz tube. The induced power used for the hydrogen plasma is 90 W. Typical plasma exposure conditions are 2h at 250°C. In order to investigate the recovery of passivated donor states and the stability of passivated deep levels, a post-hydrogenation annealing was carried out in H_2 ambient or AsH_3 ambient at 450°C.

2. 2. 3 Methods for characterization of GaAs epilayer on Si

Carrier concentration profiles are obtained by electrochemical capacitance voltage measurement using a Polaron model PN4200 system. PL spectra are recorded at 4.2 K using a 514.5 nm Ar-ion laser as an excitation source, and a GaAs photo multiplier tube (PMT) as a detector. Deep level transient spectroscopy (DLTS) measurements are carried out using an automated (HORIBA DA 1500) system at temperatures ranging from 100 K to 400 K using a gold Schottky contacts made on GaAs epilayer surface, with AuSb/Au ohmic contacts on the back side of the Si substrate.

2.3 Characterization of hydrogen plasma passivation effects on GaAs on Si

2. 3. 1 Passivation of free carrier in GaAs on Si

The MOCVD-grown unintentionally doped GaAs epilayer grown on Si substrate usually has a high carrier concentration mainly due to the Si auto diffusion from the substrate. Figure 2.3 (a) shows free-electron depth profiles of the n-type samples (Si) obtained from the C-V profiles which

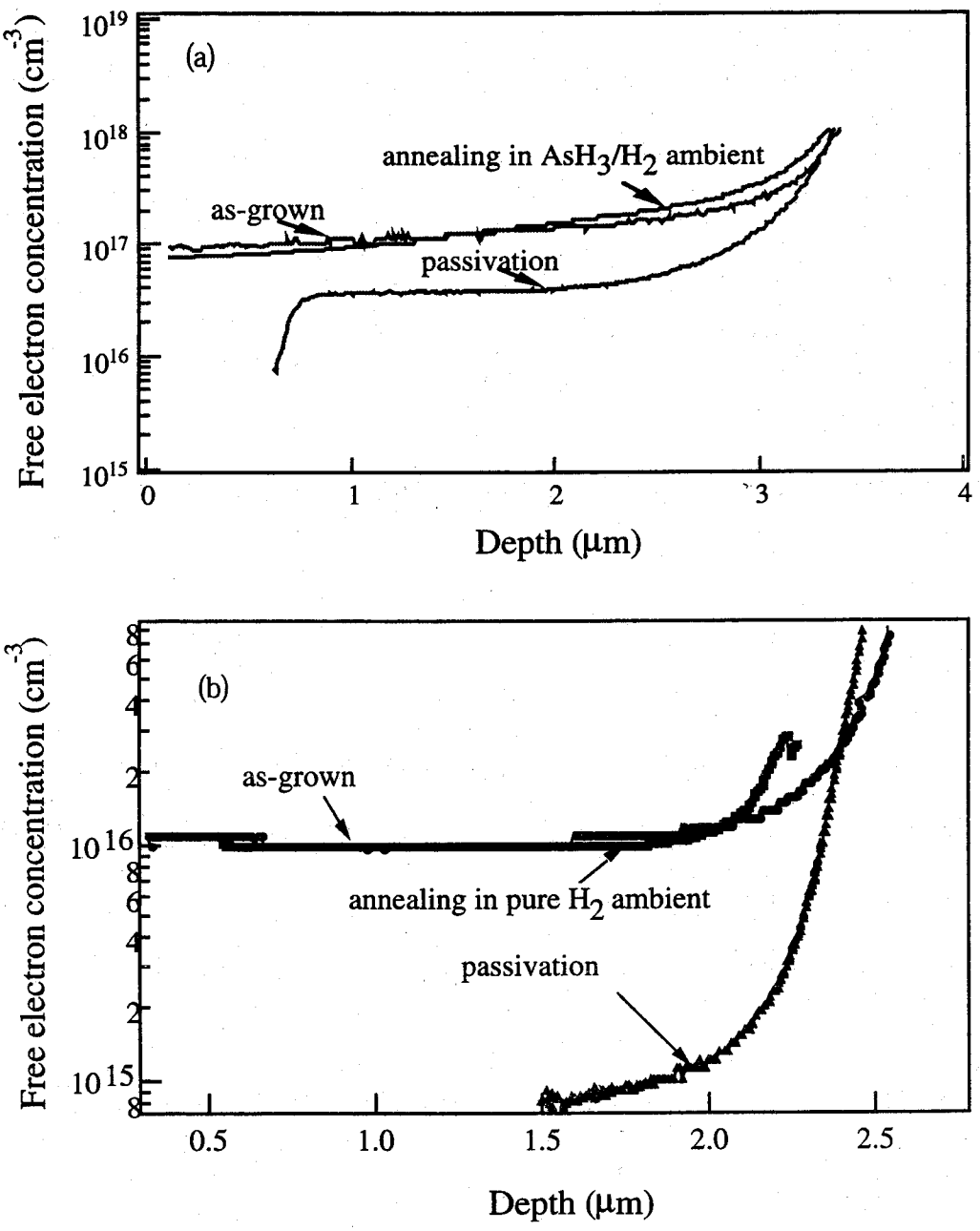

Fig. 2. 3 Free-electron concentration depth profiles of (a) as-grown, H_2 plasma passivated and annealed in AsH_3/H_2 ambient, (b) as-grown, H_2 plasma passivated and annealed in pure H_2 ambient,unintentionally doped GaAs epilayers on Si.

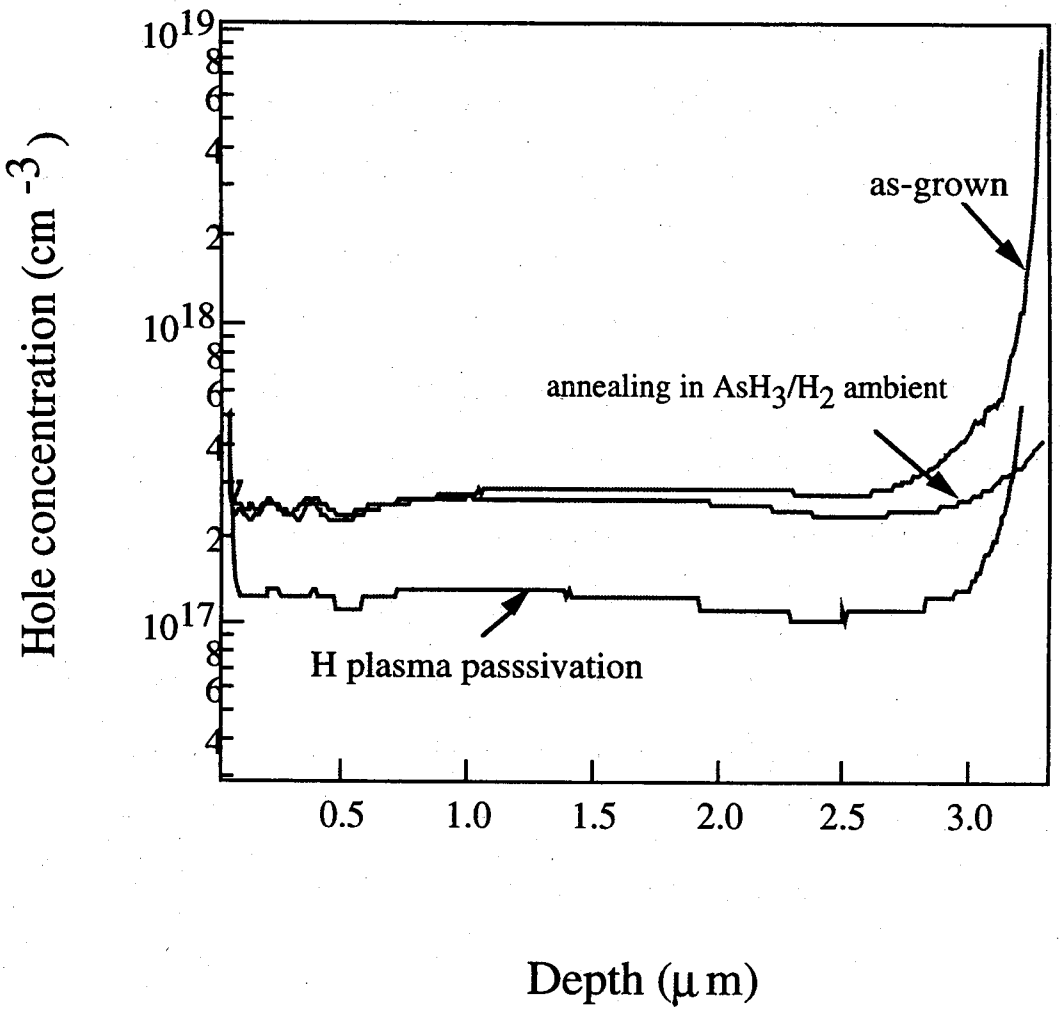

Fig. 2. 4 Free-hole concentration depth profiles of as-grown, H_2 plasma passivated and annealed in AsH_3/H_2 ambient p-type GaAs (Zn) epilayers on Si.

are taken before and after hydrogen plasma exposure, and after post hydrogenation annealing at 450°C for 10 min AsH_3/H_2 (10%) ambient. By comparing the electrochemical C-V profiles of as-grown and passivated samples, it can be seen that the electron concentration decreases dramatically after the hydrogen plasma passivation process. The carrier concentration of the reference sample (as-grown) is 1×10^{17} cm^{-3} throughout the 3 μm thick layer, whereas the hydrogenated sample shows a reduced carrier concentration throughout the thickness. This suggests neutralization of the Si donor due to hydrogen exposure. The activity of the donor was completely restored after annealing at 450°C for 10 min in AsH_3/H_2(10%) ambient. For comparison, another sample grown at a low temperature with a carrier concentration of 1×10^{16} cm^{-3} was also passivated in H_2 plasma and then annealed in pure H_2 ambient. As shown in Fig. 2.3 (b), the activity of the donor was also completely restored after annealing at 450°C for 10 min in pure H_2 ambient. It means that there is no difference in the recovery of carrier concentration between the H_2 annealing and AsH_3 annealing. Fig. 2.4 shows free-hole depth profiles of the p-type GaAs/Si (Zn). Just like free electron in n-type sample, the electrical activity of hole was significantly passivated by H atoms incorporation. However, the activity of the acceptor was completely restored after annealing at 450°C for 10 min in AsH_3/H_2 ambient. These results are consistent with previous description by Chevalier etal.[12].

2. 3. 2 Photoluminescence study

The 4.2 K PL spectra are shown in Fig. 2. 5 for the three samples, (a) as-grown, (b) H_2 plasma passivated and (c) H_2 plasma passivated and then annealed in AsH_3 ambient. Three dominant peaks appeared for the as-grown samples, heavy hole associated free exciton peak B (1.485 meV), carbon impurity bound exciton peak C (1.469 meV) and recombination peak D (1.455 meV) of bound exciton to deep defect center. Besides peaks B, C, D, and E (1.42 meV), peak A (1.50 meV) is also weakly observed after H_2 plasma passivation. Peak A is attributed to excitons associated with

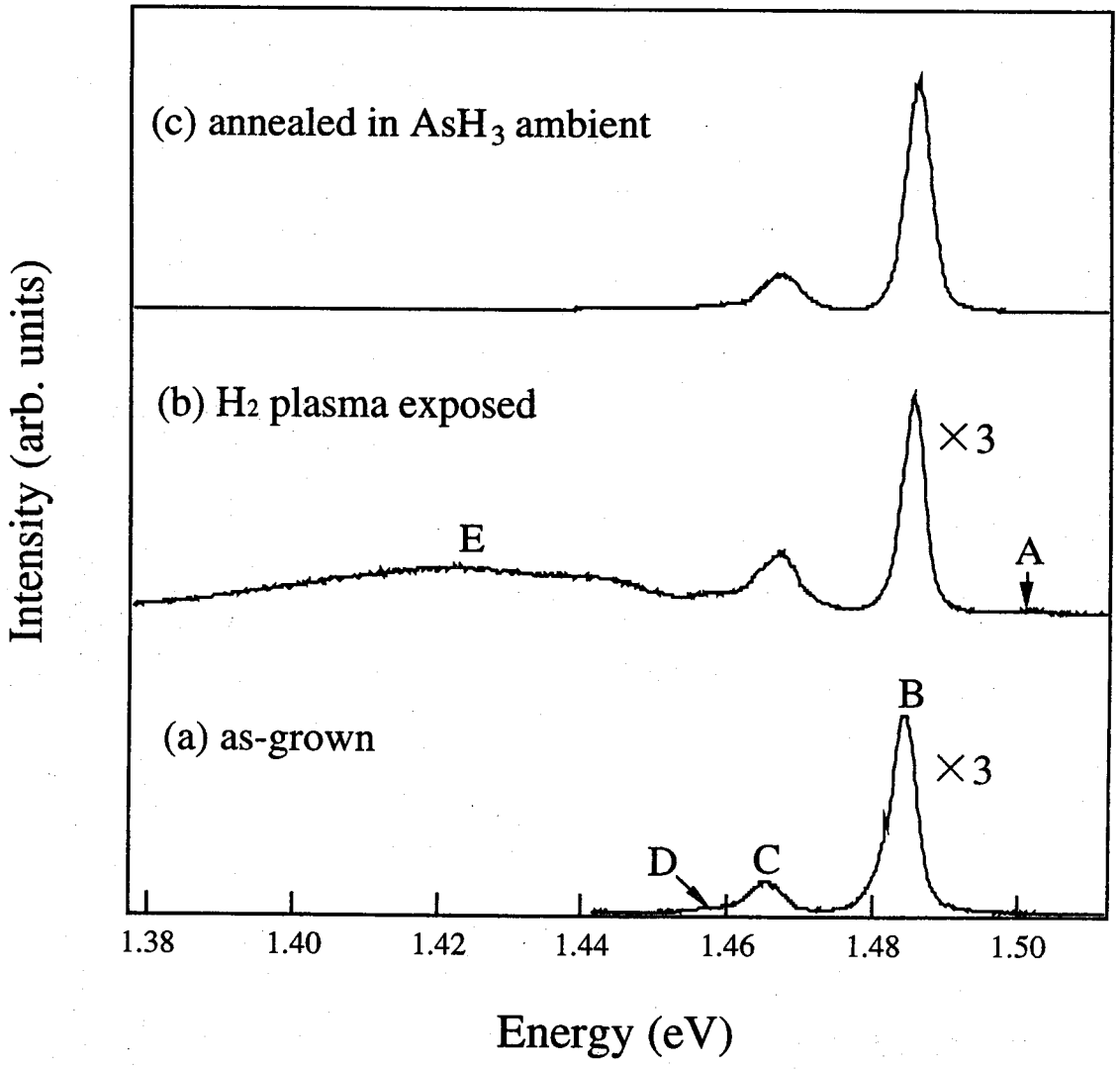

Fig. 2. 5 The PL spectra of as-grown, passivated and AsH_3 annealed passivated GaAs epilayers on Si recorded at 4.2 K.

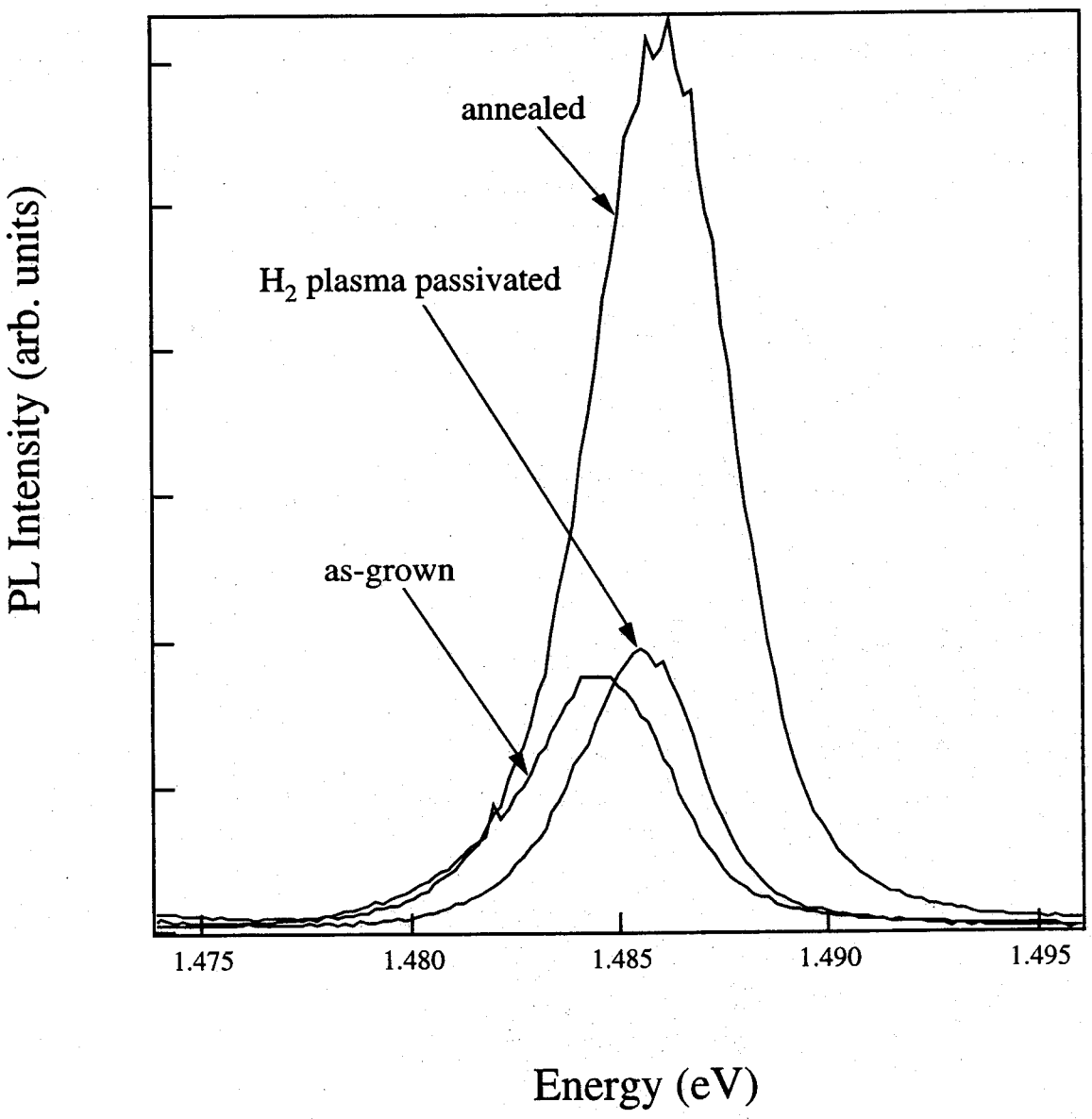

Fig. 2. 6 The enlarged plot of the main emission peak B shown in Fig. 2. 5.

light holes.[13] Broad emission band E around 1.42 eV may be due to the emission from an acceptor level related to As atom vacancies which are produced by H plasma exposure.[14] Comparing the two PL spectra, the FWHM of peak B is decreased from 4.03 meV to 3.44 meV after passivation, which may be due to passivation of nonradiative recombination centers such as dislocations, or large decrease in carrier concentration by passivation. As a result, passivation reduces the perturbation of the band edge via deformation potential, via coulomb interaction, and by forming a band of impurity states. The intensity of peak B after passivation only shows a little increase, though the carrier concentration has decreased and some electrical activity of deep defects was passivated. Since the intensity of free exciton emission is supposed to increase with passivation. However, almost no increase in the emission peak with passivation suggests that other recombination channels have been made during H plasma exposure induced damages (peak E). When the passivated samples are annealed under a sufficient As vapor pressure, the peak E disappears, and the intensity of PL signal is as large as four times than the as-grown samples while the FWHM (3.82 meV) of peak B is still less than the as-grown samples, the quality of GaAs on Si epilayers are strongly improved. The results further confirm that the improvement in PL properties is due to the passivation of deep recombination centers such as the dislocations and defects.

Figure 2. 6 shows the enlarged plot of the main emission peak B in figure 2. 5. It can be clearly seen that PL peak wavelength are different for three samples and are blue-shifted compared to the as-grown sample. As possible physics, two possible reasons can be suggested to explain this blue-shift: (i) decrease of tail states associated with defects, which will result in blue-shift of the peak and narrower spectra, and (ii) change of the residual strain related to different concentration of hydrogen and defects.

2. 3. 3 Passivation of the deep levels in GaAs on Si

It is very interesting to investigate the change of deep level concentration as the passivation is completed, since the minority carrier lifetime of GaAs on Si epilayers can be controlled by the existence of nonradiative recombination centers.[14] Figure 2.7 shows the results of the DLTS measurement carried out for the as-grown sample which are are presented $C(t_1)$ - $C(t_2)$ vs. T. For each temperature at which a peak occurs, an emission rate $e_n(T_m)$ is calculated from Eq. (2.1),

$$e_n(T_m) = \frac{\ln(t_2/t_1)}{(t_2 - t_1)} \tag{2.1}$$

and the values of $e_n(T_m)/T_m^2$ are then plotted vs. T_m^{-1}. The slopes of these Arrhenius plots give values of the effective trap depth E_T using Eq.(2.2).

$$\ln\frac{e_n}{T^2} = \ln\left[16\pi m_n^* k^2 h^{-3}(g_0/g_1)e^{\alpha_T/k}\sigma_{n\infty}\right] - \frac{E_T}{k}\frac{1}{T} \tag{2.2}$$

For GaAs, the constant $16\pi m_n^* k^2 h^{-3} = 2.0\times10^{20} s^{-1}cm^{-2}K^{-2}$. It is also seen that the capture cross section $\sigma_{n\infty}$ can , in principle, be determined from the intercept (at T^{-1}=0) of the $e_n(T_m)/T_m^2$ vs. T_m^{-1} plot, since g_0/g_1 and $e^{\alpha_T/k}$ may already be known and, in any case, are usually of the order of unity. However, there is a danger here, because a slight error or uncertainty in E_T can lead to a large error in $\sigma_{n\infty}$, since it is in a ln term.

As shown in Fig. 2. 8, we have analyzed the main peaks ED1 and EL2 using Arrhenius plot and obtained an activation energy of 0.44 eV for ED1which is similar to the result reported by our group. This electron trap is attributed to Si-dislocation complex which has a distributed energy centered at around 0.44 eV.[15] On the other hand, another main deep level EL2 with an activation energy of 0.73 eV was obtained, which was attributed to the EL2 family.

The deep level concentration can be calculated using Eq.(2.3).

$$N_T = 2\left\{\frac{\Delta C(0)}{C(\infty)}\right\}N_D \tag{2.3}$$

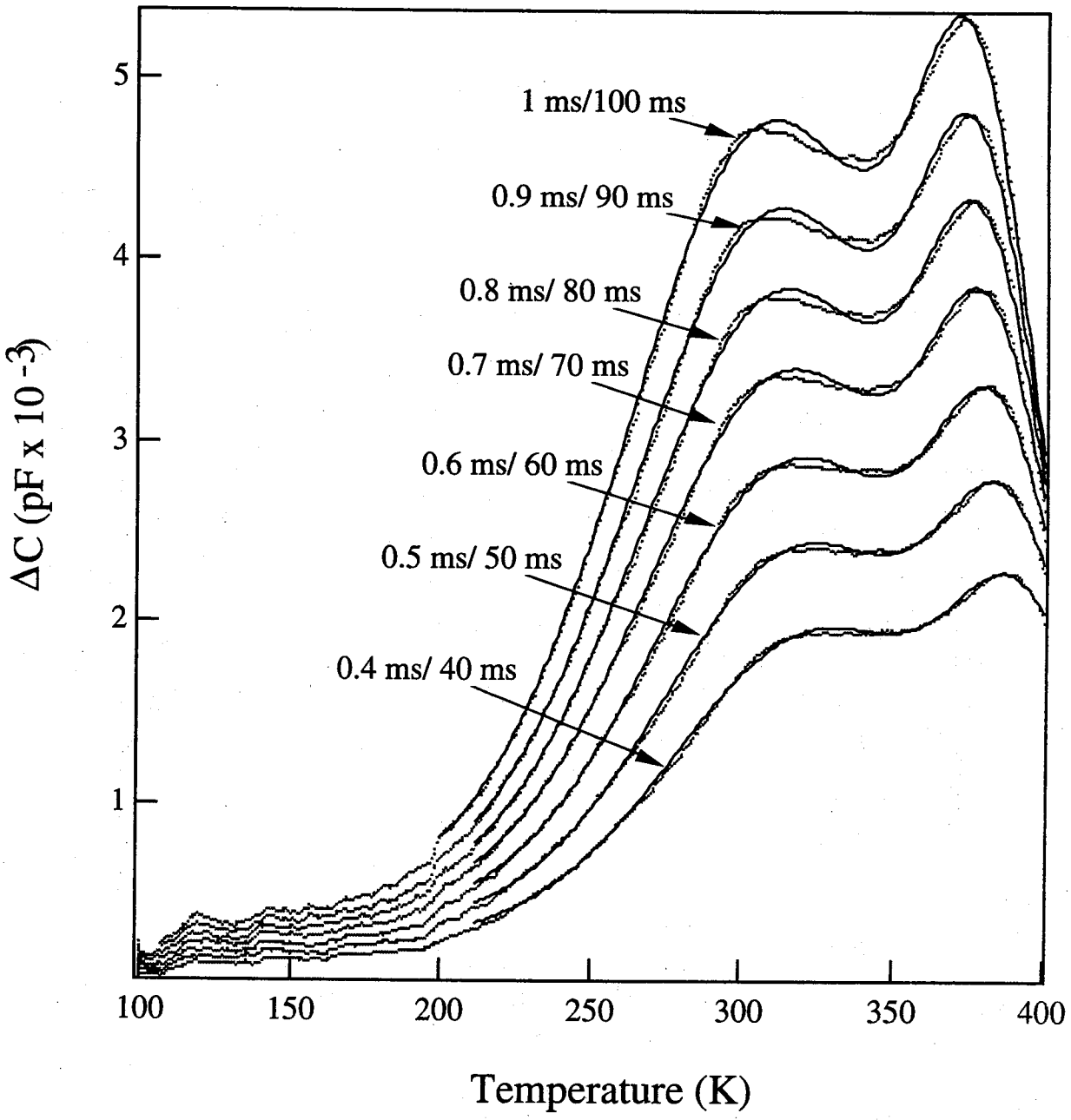

Fig. 2. 7 DLTS spectra for as-grown GaAs eplayer on Si, the solid lines are the fitted results.

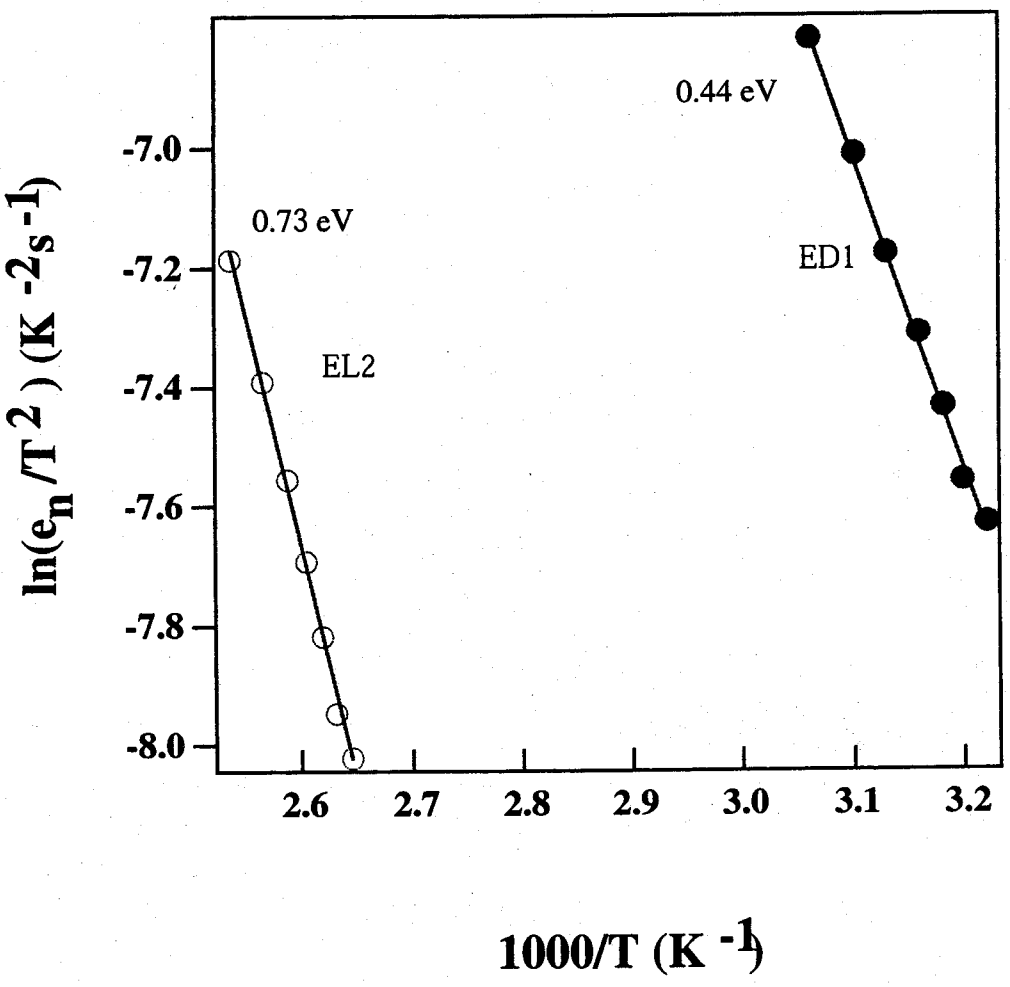

Fig. 2. 8 Arrhenius plots of thermal emission rates deduced from DLTS spectra as shown in Fig. 2. 7.

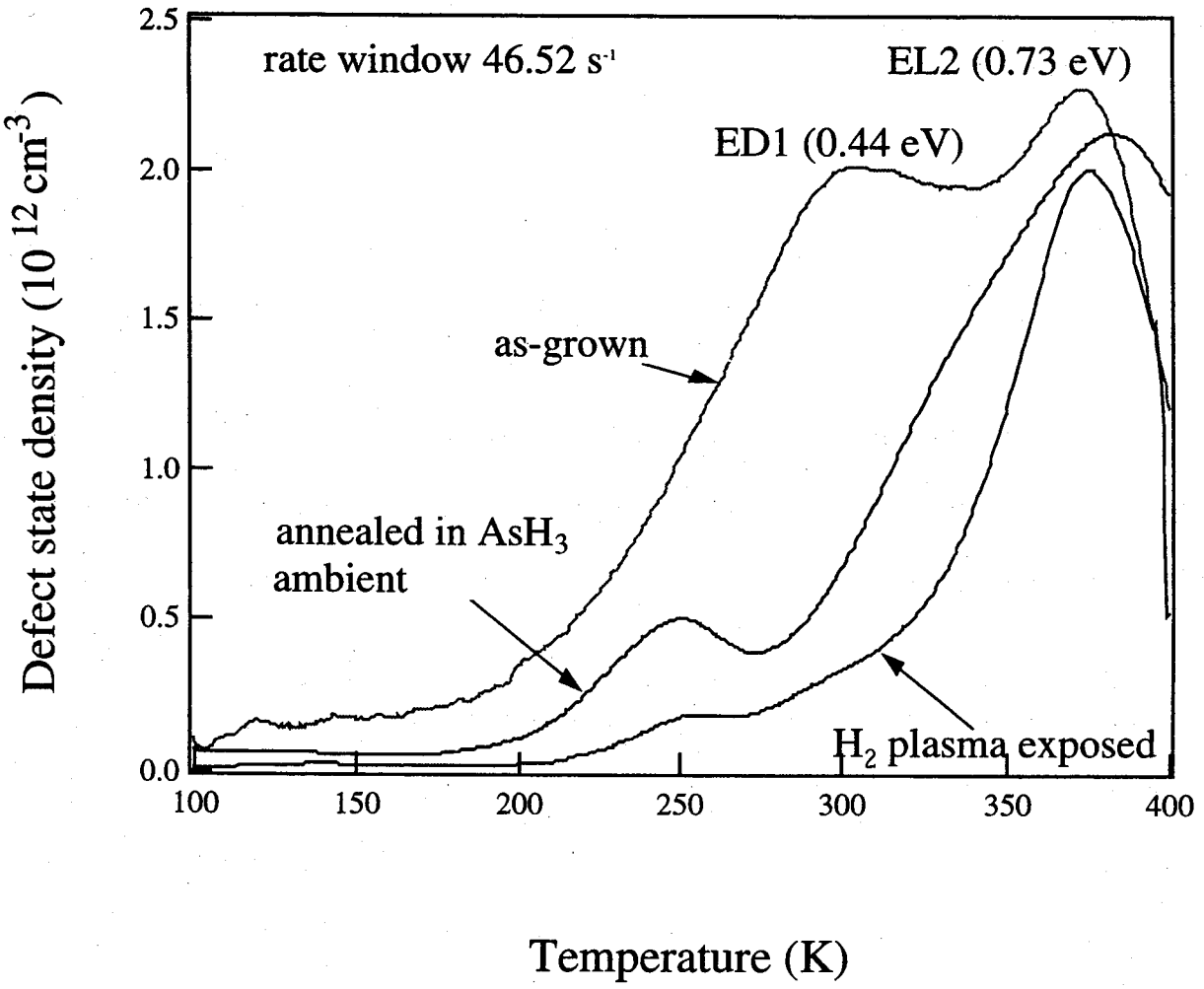

Fig. 2. 9 DLTS spectra for as-grown, passivated and annealed in AsH_3/H_2 ambient passivated GaAs epilayers on Si.

Here, the value of carrier concentration N_D can be calculated from C-V characteristics. $\Delta C(0)$is the value of $\Delta C(t)$just after the pulse voltage is off ($\Delta C(t) = C(\infty) - C(t)$).

$$\Delta C(0) = \frac{\left|\Delta C(t_2) - \Delta C(t_1)\right|_{T=T_m}}{\exp\left(-\frac{t_2}{\tau_m}\right) - \exp\left(-\frac{t_1}{\tau_m}\right)} \tag{2.4}$$

where

$$\tau_m = \frac{1}{e_n(T_m)} = \frac{t_2 - t_1}{\ln\left(\frac{t_2}{t_1}\right)} \tag{2.5}$$

Also, can be seen from Fig. 2. 9, the decrease in deep level concentration is clearly seen after H plasma passivation, especially, the thermal emission band of deep level around 300 K (ED1) which is almost vanished, and deep level passivation effect still persists after dehydrogenated in AsH_3 (10%) ambient at 450°C. These results further confirm that the PL properties and minority carrier lifetime are improved by passivation of the dislocation-related deep levels. However, almost no decrease of EL2 was observed after H_2 plasma passivation. It suggests that some H_2 plasma-induced damages negated the passivation effects of EL2 which is related to anti site As_{Ga} defect complex.

2. 4 Photoluminescence study of hydrogen plasma passivated AlGaAs/GaAs MQW on Si

Growth and fabrication of quantum well and vertical-cavity surface-emitting lasers (VCSEL) on Si substrates have been extensively studied, because of their potential application for optical interconnections in future optoelectronic integrated circuits (OEIC). However, high dislocation density (~10^6 cm^{-2}) in the GaAs epilayer grown on Si substrate (GaAs/Si), prevents the long lifetime operation of MQW lasers and stable continuous wave (cw) operation for VCSEL on Si

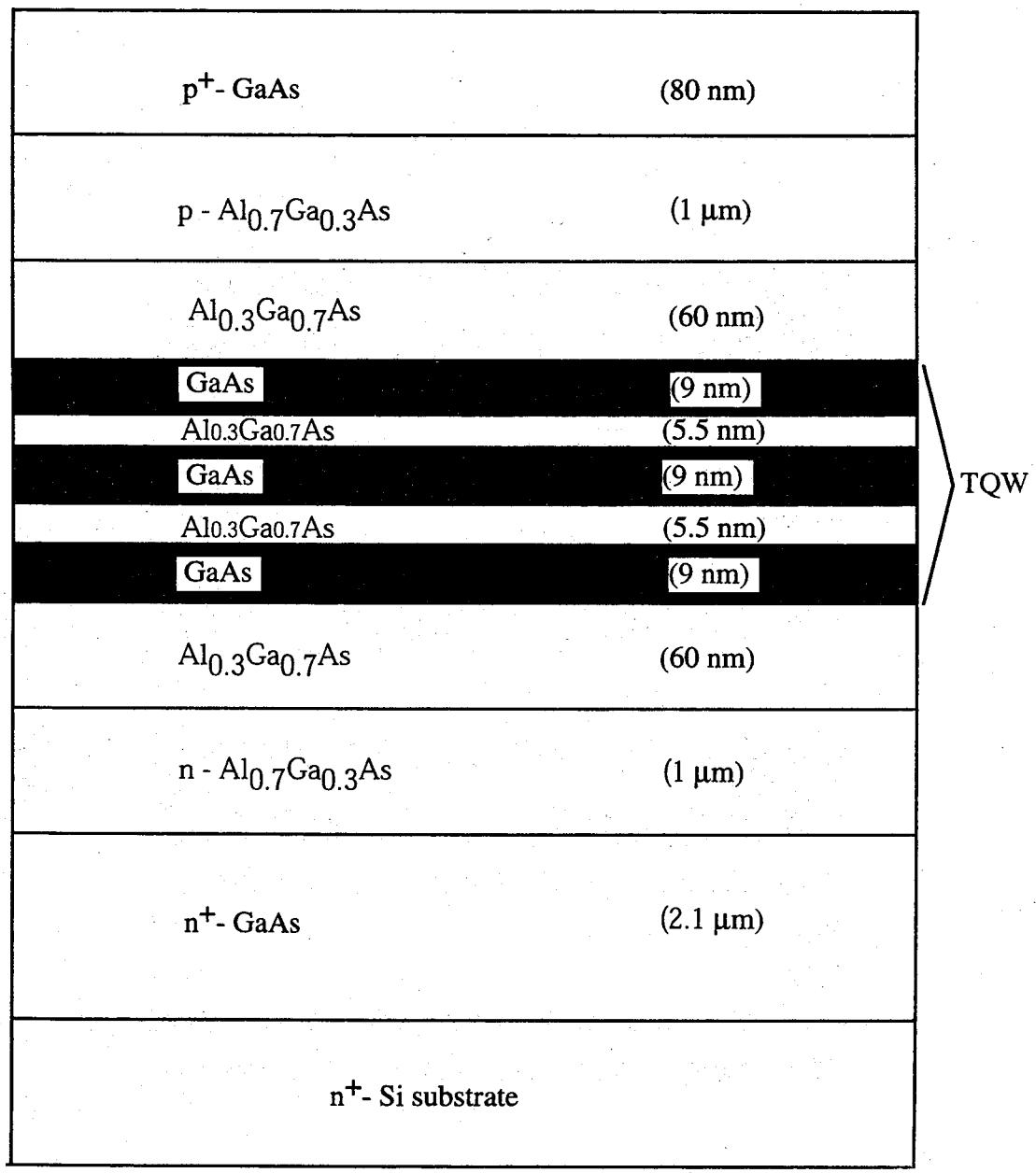

Fig. 2. 10 Schematic view of the 3 pairs $Al_{0.3}Ga_{0.7}As$ (5.5 nm)/GaAs (9 nm) MQW structure on Si.

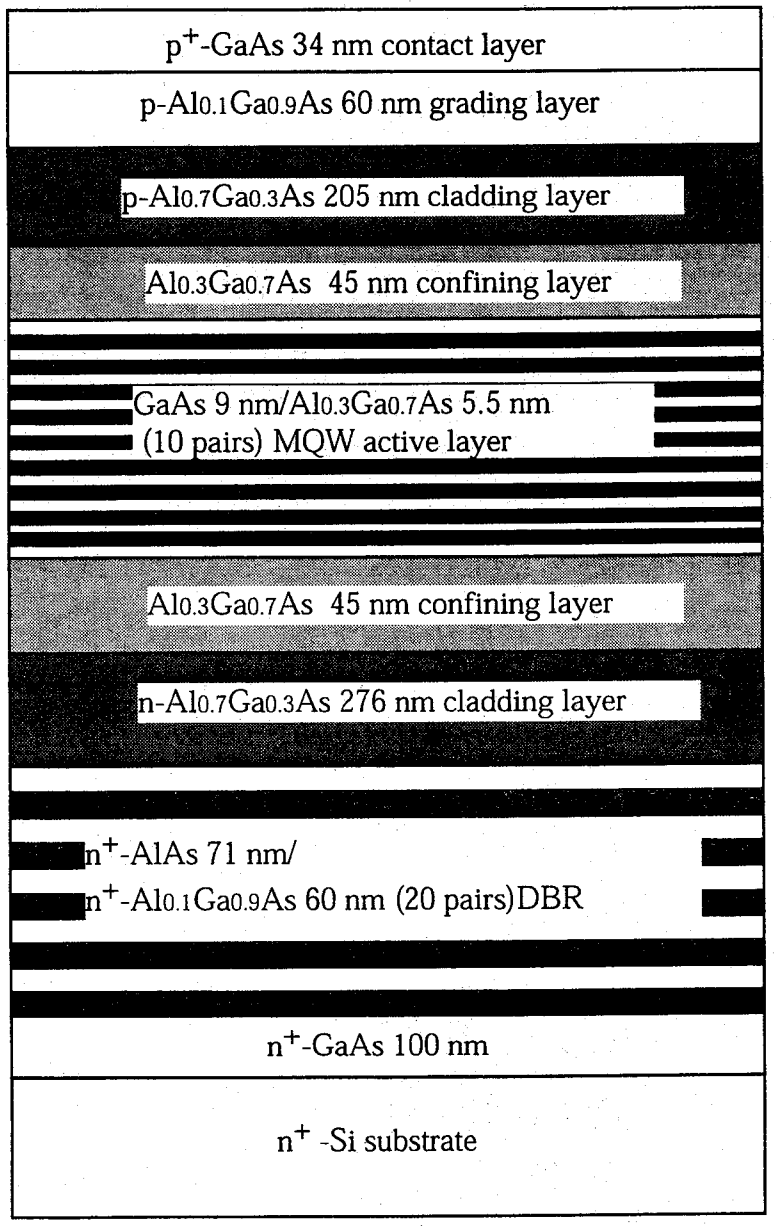

Fig. 2. 11 Schematic view of AlGaAs/GaAs MQW VCSEL structure on Si substrate.

substrates at room temperature until now[16]. Since the generation of defects in GaAs/Si epilayers can not be avoided to the full extent, passivation of the electrical activity of these defects is becoming very essential. In this section, we present the passivation effects of H plasma exposure on the $Al_{0.3}Ga_{0.7}As$/GaAs MQW laser structure and VCSEL structure consisting of $Al_{0.3}Ga_{0.7}As$/GaAs MQW active layer and $Al_{0.1}Ga_{0.9}As$/AlAs distributed Bragg reflector (DBR) grown on Si substrates by photoluminescence (PL) measurement. It was found that the H plasma exposure significantly increased photluminescence emission intensity and quantum efficiency at the MQW active layer.

2. 4. 1 Fabrication of AlGaAs/GaAs MQW and VCSEL structures on Si

In this experiment, two type laser structure was grown on n^+-Si substrate oriented 2° off (100) towards [011] by metalorganic chemical vapor deposition (MOCVD) at atmospheric pressure. As shown in Fig. 2. 10, for the MQW laser structures, the 3 pairs $Al_{0.3}Ga_{0.7}As$ (5.5 nm)/GaAs (9 nm) MQW sandwiched by $Al_{0.7}Ga_{0.3}As$ cladding layer was grown on a 2.1 μm GaAs buffer layer on Si substrate at 750°C using two step growth method. A 34 nm thick GaAs contact layer was grown at the surface. As shown in Fig. 2. 11, for a VCSEL structures, a 20 pairs $Al_{0.1}Ga_{0.9}As$ (60 nm)/AlAs (71 nm) DBR was first grown Si substrate. Then the 10 pairs $Al_{0.3}Ga_{0.7}As$ (5.5 nm)/GaAs (9 nm) sandwiched by $Al_{0.7}Ga_{0.3}As$ cladding layer MQW-VCSEL structures layers was grown on it. Finally, a 60 nm thick $Al_{0.1}Ga_{0.9}As$ grading layer followed by a 34 nm thick GaAs contact layer was grown at the surface. The source materials for Ga and As were trimethylgallium (TMG), trimethylallumium (TMA) and AsH_3, respectively. Diethylzinc (DEZ) and H_2Se were *p*-type and *n*-type dopants, respectively. The resonant-mode wavelength of the Fabry-Perot cavity in VCSEL structure was designed to laser at 870 nm at room temperature. After the epitaxial growth, the wafers were cleaved into 5-7 mm square. Sample A was left in the as-grown state. Sample B was subjected to a radio-frequency (13.56 MHz) H plasma. The passivation was carried out in a quartz

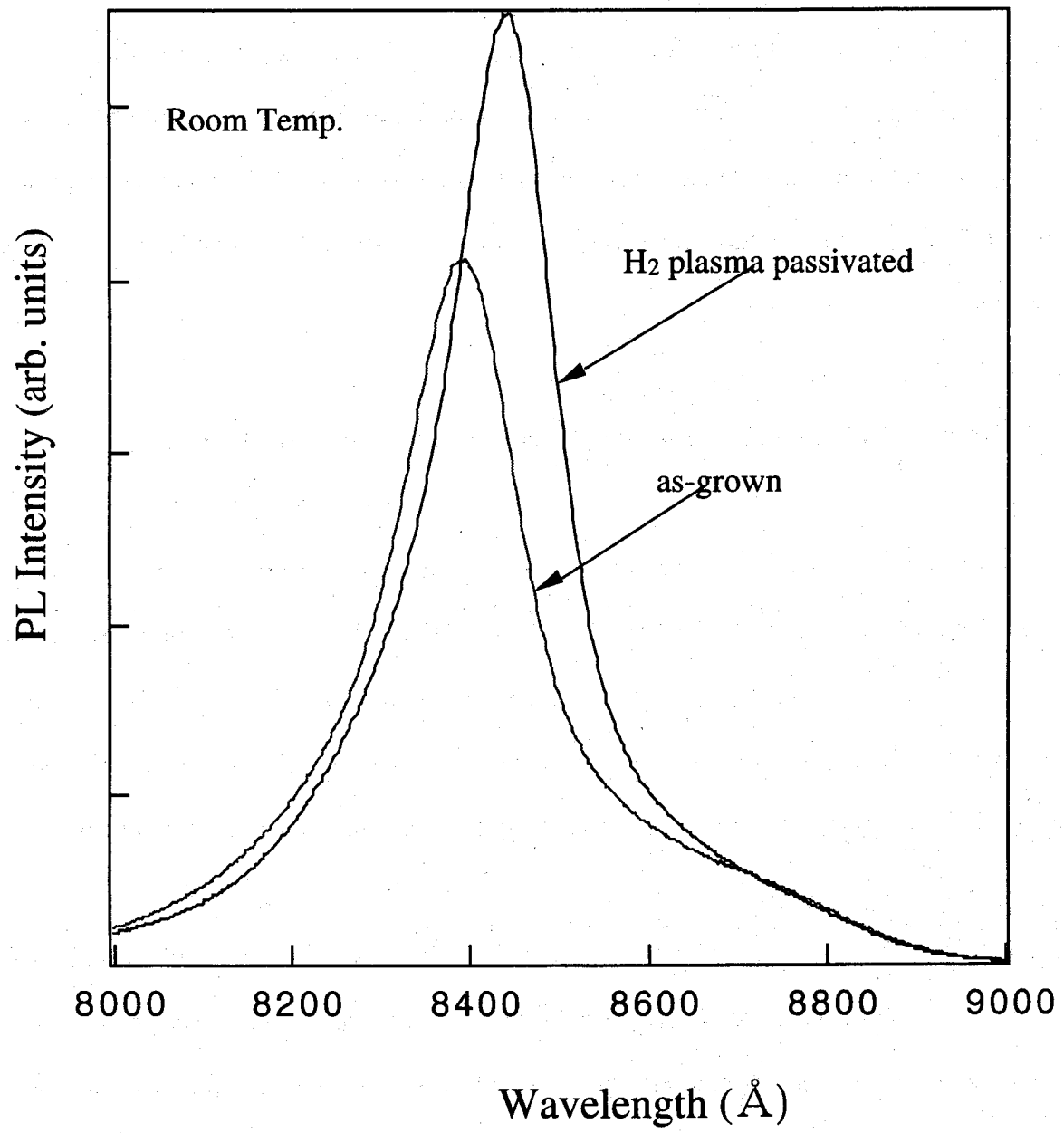

Fig. 2. 12 Room temperature PL spectra of the as-grown and hydrogen plasma passivated $Al_{0.3}Ga_{0.7}As$/GaAs MQWs on Si.

tube at 0.1 Torr, 250°C for 1 hour. The input power used for the plasma was 90 W. PL spectra were recorded at 77 K and room temperature (300 K), respectively

2. 4. 2 Characterization of AlGaAs/GaAs MQW on Si

Room temperature PL spectra from the as grown sample of 3 pairs $Al_{0.3}Ga_{0.7}As$/GaAs MQWs on Si and after hydrogenation is shown in Fig. 2. 12. The improvement in PL intensity from the MQWs is clearly seen. It may further be seen from this figure that is a appreciable decrease in the spectral width of emission from MQW on hydrogenation. This observation on improvement in PL signal with change in spectra width suggests that hydrogenation passivates the defects in the core of QW on Si and the interface feature responsible for line broad are also influenced by hydrogenation[17].

2. 4. 3 Characterization of AlGaAs/GaAs VCSEL on Si

The room temperature PL spectra are shown in Fig. 2. 13 for AlGaAs/GaAs MQW VCSEL on Si before and after hydrogen plasma passivation, respectively. Two emission peaks were observed for both samples: peak A (866.4 nm) and peak B (817.2 nm). Because the emission wavelength of peak A was very near the designed resonant-mode wavelength of the Fabry-Perot cavity (870 nm), peak A was recognized as the DBR reflection PL peak of the VCSEL. Peak B was originated from the recombination emission of the $Al_{0.1}Ga_{0.9}As$ top grading layer. After H plasma passivation, the intensity of the cavity mode peak (peak A) was enhanced as large as 3 times. However, almost no increase was observed for peak B, it seemed that some plasma induced damages negated the beneficial effects of H atoms incorporation in the surface region.[18] As a result, the integrated intensity of the room temperature luminescence was greatly increased only by the increased DBR reflection PL emission. The excitation power dependencies of peak A were shown in Fig. 2. 14. It

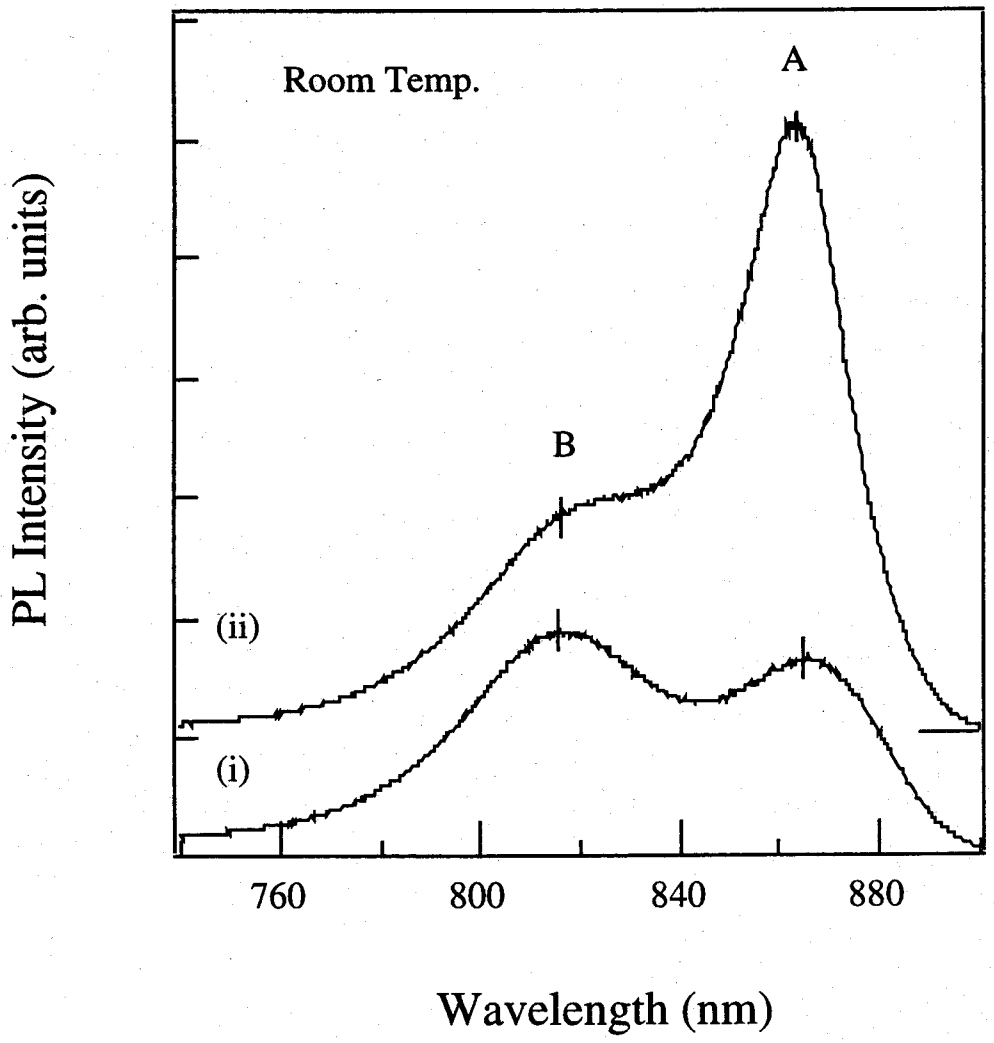

Fig. 2.13 The room temperature PL spectra for AlGaAs/GaAs MQW VCSEL on Si (i) before and (ii) after hydrogen plasma passivation, respectively.

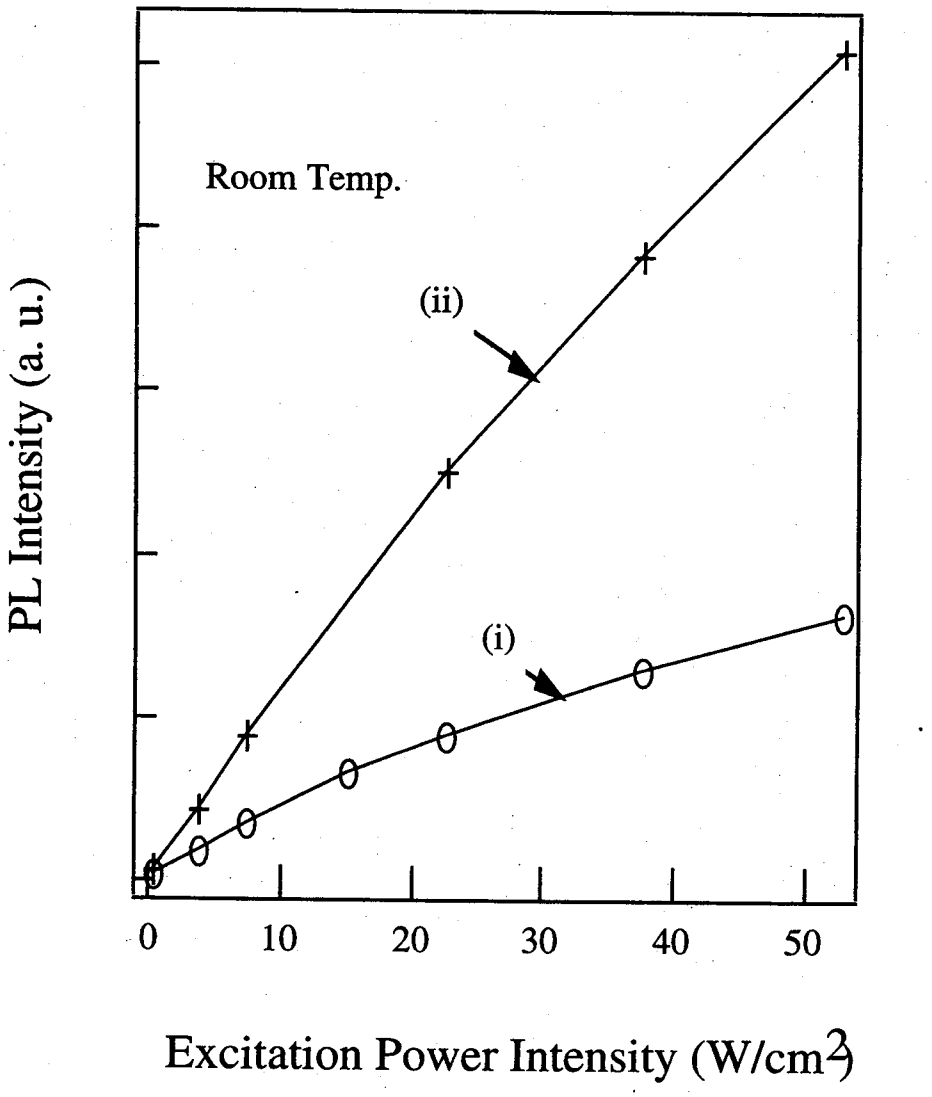

Fig. 2. 14 The excitation power dependencies of room temperature cavity mode emission intensity for AlGaAs/GaAs MQW VCSEL on Si (i) before and (ii) after hydrogen plasma passivation, respectively.

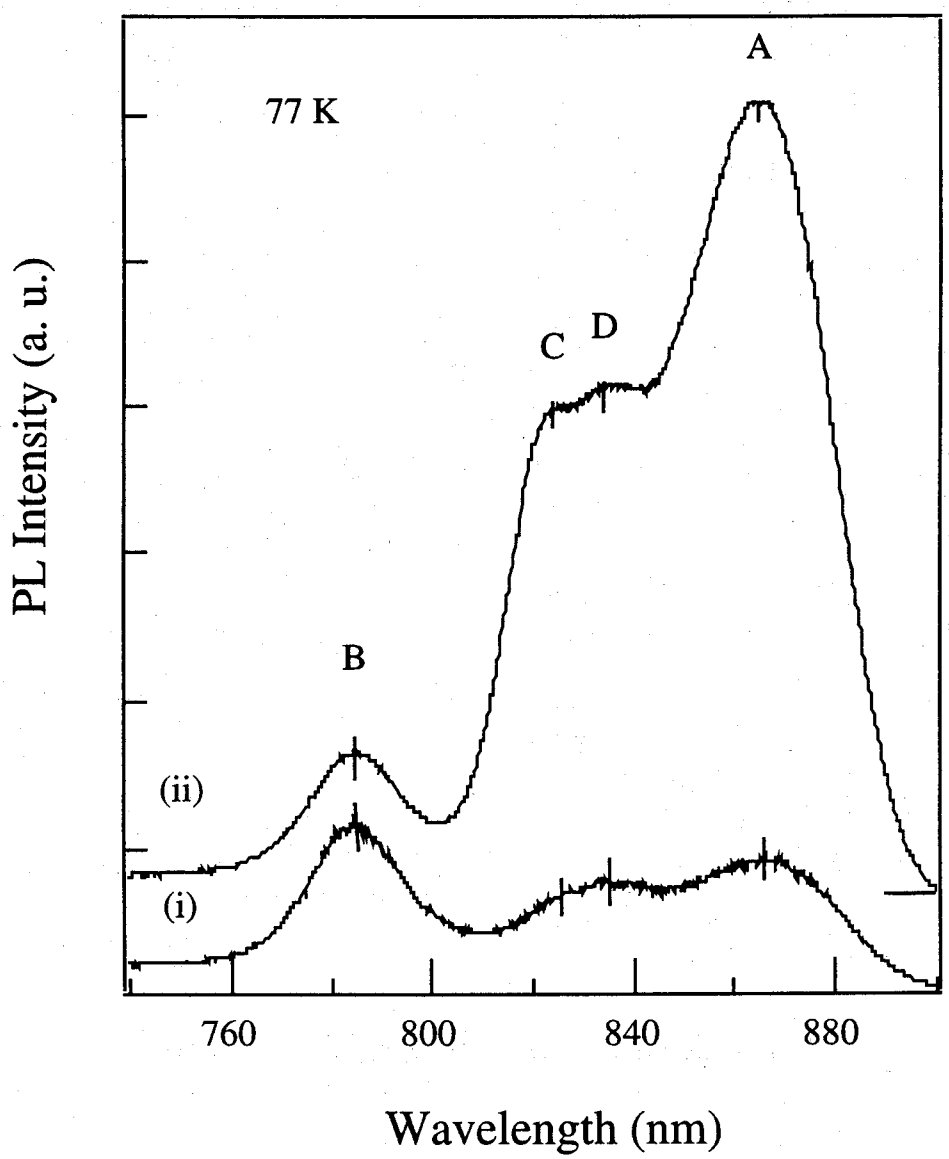

Fig. 2. 15 77K PL spectra for AlGaAs/GaAs MQW VCSEL on Si before and after hydrogen plasma passivation, respectively.

should be mentioned that the spectra shape did not change when the excitation power was increased from 6 to 700 mW, indicating that the spontaneous emission was the dominant recombination process and the stimulated emission was negligibly small, even though the MQW and the DBR reflection PL emission were in resonance at room temperature. Just like efficient diodes, from Fig. 2. 14, we can see that the quantum efficiency of the H_2 plasma passivated $Al_{0.3}Ga_{0.7}As$/GaAs VCSEL on Si substrate was increased as large as 3 times compared with that of the as-grown sample at room temperature.

The low temperature (77 K) PL spectra are shown in Fig. 2. 15. Since the cavity mode was not designed to be equal to the MQW wavelength at this temperature, both the splitted MQW emission peaks C (824.6 nm: heavy hole related emission), D(834.8: heavy hole related emission)[19] and the cavity mode emission peak A (865.6 nm) were observed. The separation of the MQW and DBR reflection peaks was attributed to the fact that the MQW peak shifts to shorter wavelength faster than the cavity mode peak with decreasing the temperature[20]. In addition, the wavelength of $Al_{0.1}Ga_{0.9}As$ top layer emission peak B was shifted to 785.2 nm. It can be seen that the PL intensity of MQW peaks (peaks C and D) of the H plasma passivated sample were dramatically increased as large as 6 times compared to that of the as-grown sample. As a result, the DBR reflection emission peak A was enhanced as the same order. This directly proved that the enhancement of spontaneous emission from VCSEL structure by H plasma passivation was dominantly attributed to the passivation effects on the nonradiative recombination centers which enhanced the MQW exciton emission.

2. 5 Conclusion

In summary, we have demonstrated a significant improvement in the optical and electrical properties of GaAs on Si by H plasma passivation followed by annealing in AsH_3 ambient. Both the shallow and deep states in GaAs/Si epilayers were effectively passivated by H_2 plasma passivation. The properties of PL or bulk and MQW materials on Si was obviously improved, and are attributed to the passivation of the defects-related deep recombination centers. The passivation effect of Si-dislocation complex (0.44 eV) still persists even after 450°C dehydrogenation process, which is the usual process temperature. This result also suggests that the H plasma passivation may be a useful way to improve the properties of GaAs devices grown on Si substrates.

References:

1) T. Soga, T. Kato, M. Yang, T, Jimbo and M. Umeno, J. Appl. Phys. **78** (1995) 4196 .

2) T. Egawa, H. Tada, Y. Kobayashi, T. Soga, T. Jimbo and M. Umeno, Appl. Phys. Lett. **57** (1990) 1179.

3) S. F. Fang, K. Adomi, S. lyer, H.Morkoc, H.Zabel, C. Choi and N. Otsuka, J. Appl. Phys. **68** (1990) R31.

4) M.Akiyama, Y.Kawarada and K.Kaminishi, J. Crystal Growth **68** (1984) 21.

5) K.Nozawa and Y.Horikoshi, Jpn. J. Appl. Phys. **30** (1991) L668.

6) M.Yamaguchi, A.Yamamoto, M.Tachikawa, Y.Itoh and M.Sugo, Appl. Phys. Lett. **53** (1988) 2293 .

7) S. J. Pearton, W. C. Dautremont-Smith, J. Chevallier, C. W. Tu and K. D. Cummings, J. Appl. Phys. **59** (1986) 2821.

8) B. Chatterjee and S. A. Ringel, J. Appl. Phys. **77** (1995) 3885.

9) S. J. Pearton, J. W. Corbett and M. Stavola, *Hydrogen in Crystalline Semiconductors* (Springer, Berlin, 1992).

10) S. J. Pearton, C. S. Wu, M. Stavola, F. Ren, J. Lopata, W. C. Dautremont- Smith, S. M.Vernon and V. E. Haven, Appl. Phys. Lett. **51** (1987) 496.

11) J. M. Zavada, S. J. Pearton, R. G. Wilson, C. S. Wu, Michael Stavola, F. Ren, J. Lopata, W. C. Dautremont-Smith and S. W. Novak, J. Appl. Phys. **65** (1989) 347.

12) J. Chevallier, W. C. Dautremont- Smith, C. W. Tu and S. J. Pearton, Appl. Phys. Lett. **49** (1985) 406.

13) V. Alberts, Jpn. J. Appl. Phys. **33** (1994) 611.

14) T. Soga, T. Jimbo and M. Umeno, Jpn. J. Appl. Phys. **33** (1994) 1494.

15) T. Soga, S. Sakai, M. Umeno and S. Hattori, Jpn. J. Appl. Phys, **25** (1986) 1510.

16) Y. Murata, N. Nakanishi, T. Egawa, T. Jimbo, and M. Umeno, Jpn. J. Appl. Phys. **35** (1996) L1631.

17)D. Bimberg, D. Mars, J. N. Miller, R. Bauer and D. Oertel, J. Vac. Sci. Technol. B **4** (1986) 1014.

18) P. Friedel and S. Gourrier, Appl. Phys. Lett. **42** (1983) 509.

19) C. Jagannath, S. Zemon, P. Norris, and B. S. Elman, Appl. Phys. Lett., **51** (1987) 1268.

20)Y. Hanamaki, H. Akiyama, and Y. Shiraki, Semicond. Sci. Technol., **14** (1999) 797.